Quantum optical effective-medium theory for loss-compensated metamaterials Supplementary Material

Ehsan Amooghorban,[1,2,3] N. Asger Mortensen,[1] and Martijn Wubs[1,*]

[1]*Department of Photonics Engineering, Technical University of Denmark, DK-2800 Kgs. Lyngby, Denmark*
[2]*Department of Physics, Shahrekord University, Shahrekord, Iran*
[3]*Department of Physics, University of Isfahan, Isfahan, Iran*

(Dated: February 8, 2013)

In this supplementary material, it is shown that the usual effective-medium theory breaks down for loss-compensated metamaterials, and our quantum optical effective-medium theory is accurate, also when using measured values for dielectric functions of gain and loss materials. We thus observe the same qualitative behavior as for the simple single-Lorentzian dielectric functions used in the main text. This supports our claim that we identify a fundamental issue about loss compensation in quantum optics that has observable consequences.

I. EXPERIMENTAL PARAMETERS FOR GAIN AND LOSS

In the main text, we focused on the fundamental issue of loss compensation in quantum optics. To keep the presentation simple and the number of parameters small, we studied multilayer structures and assumed that the gain and loss layers were equally thick, both described by single-resonance Lorentzian dielectric functions, with gain and loss almost equally strong in neighboring layers. In this supplement, we consider layers of a pumped dye medium alternating with layers of silver. We use dielectric functions that are fitted to experimental values, for both types of layers. We thereby show that the fundamentally interesting quantum optical breakdown of effective-index theory for loss-compensated metamaterials as discussed in the main text has experimental relevance.

A. Gain medium

The active medium considered in the calculations of this supplement consists of a dielectric host material (of refractive index $n_{\mathrm{h}} = 1.62$) doped with rhodamine 800 (Rh800) dye molecules that qualitatively can be described by the Lorentz model [1]

$$\varepsilon_{\mathrm{g}} = \varepsilon_{\mathrm{h}} + \frac{A_{\mathrm{a}}\omega_{0a}^2}{\omega_{0a}^2 - \omega^2 - \mathrm{i}\gamma_{\mathrm{a}}\omega} + \frac{A_{\mathrm{e}}\omega_{0e}^2}{\omega_{0e}^2 - \omega^2 - \mathrm{i}\gamma_{\mathrm{e}}\omega} \tag{1}$$

where ε_{h} is the constant background value and the parameters $A_{\mathrm{a,e}}$ are macroscopic analogs of the Lorentz oscillator strength, A_{a} for absorption in the dye-doped layer and A_{a} for emission in the same layer. Indeed, A_{e} describes gain and is related to the concentration of dye molecules and to the fraction of those dye molecules in the excited state. Without pumping, $A_{\mathrm{e}} > 0$ and the dye-doped layer is lossy, but with sufficient pumping population inversion is attained and $A_{\mathrm{e}} < 0$.

The total density of dye molecules embedded in the host dielectric is assumed to be $N = 3.89 \times 10^{18}\,\mathrm{cm}^{-3}$ [2–4]. The parameters defining the response of the dye molecules are taken from published experimental data [2, 5]. In particular, the absorption and emission cross sections of each molecule have Lorentzian shapes defined by the same half-widths, $\gamma_{\mathrm{a}} = \gamma_{\mathrm{e}} = 1/(20\,\mathrm{fs})$, and are centered at $\lambda_{\mathrm{a}} = 680\,\mathrm{nm}$ and $\lambda_{\mathrm{e}} = 710\,\mathrm{nm}$, respectively. By comparing Eq. (1) with the dye relative permittivity $\varepsilon_{\mathrm{g}}(\omega_{\mathrm{a}}) = \varepsilon'_{\mathrm{g}}(\omega_{\mathrm{a}}) + \mathrm{i}\frac{c}{\omega_{\mathrm{a}}}[\varepsilon'_{\mathrm{g}}(\omega_{\mathrm{a}})]^{1/2}\alpha_{\mathrm{a}}$ and $\varepsilon_{\mathrm{g}}(\omega_e) = \varepsilon'_{\mathrm{g}}(\omega_{\mathrm{e}}) - \mathrm{i}\frac{c}{\omega_{\mathrm{e}}}[\varepsilon'_{\mathrm{g}}(\omega_{\mathrm{e}})]^{1/2}\alpha_{\mathrm{e}}$ at ω_{a} and ω_{e} [6], we find $A_{\mathrm{a}} = 0.0057$ and $A_{\mathrm{e}} = -0.0048$. Here $\varepsilon'_{\mathrm{g}}$ is the relative permittivity of the dielectric material hosting the dye molecules, and $\alpha_{\mathrm{a}} \approx \sigma_{\mathrm{a}}(\omega_{\mathrm{a}})N$ and $\alpha_{\mathrm{e}} \approx \sigma_{\mathrm{e}}(\omega_{\mathrm{e}})N$ are the absorption and gain coefficients, respectively. Furthermore, the absorption and emission cross-sections $\sigma_{\mathrm{a}} = 7.45 \times 10^{-16}\,\mathrm{cm}^2$ and $\sigma_{\mathrm{e}} = 5.78 \times 10^{-16}\,\mathrm{cm}^2$ are taken from experimental data [5].

In general the amount of gain depends on the optical local density of states, which in turn depends on the imaginary part of the dyadic Green function of the entire multilayer structure, not just of the individual amplifying layers. By

*Electronic address: mwubs@fotonik.dtu.dk

pumping, the gain and hence the dielectric function changes in the amplifying layers, whereby the Green function changes and concomitantly the LDOS. This subtle self-consistency issue is addressed in detail in Refs. 7, 8. In our work, which is focused on effective-medium theory in quantum optics, we choose to keep our model as simple as possible and for simplicity assume that the same amount of gain is achieved in all amplifying layers of the multilayer structures. To achieve this experimentally, the amplifying layers with higher LDOS would require stronger pumping [7, 8].

B. Loss medium

We assume that the gain medium alternates with thin films of silver, which is lossy. The permittivity of silver follows a Drude model corrected by two Lorentzian resonances to match experimental data at visible wavelengths [9, 10]. Thus, we describe the silver layers by the dielectric constant ε_l, which is given by [9]

$$\varepsilon_\mathrm{l} = \varepsilon_\infty - \frac{\omega_\mathrm{p}^2}{\omega^2 + \mathrm{i}\gamma\omega} + \frac{\Delta\varepsilon_\mathrm{L}\omega_\mathrm{L}^2}{\omega_\mathrm{L}^2 - \omega^2 - \mathrm{i}\gamma_\mathrm{L}\omega}. \tag{2}$$

In our numerical calculations we use $\varepsilon_\infty = 4.6$, $\omega_\mathrm{p}/\omega_0 = 13.68$, $\gamma/\omega_0 = 0.1064$, $\omega_\mathrm{L}/\omega_0 = 7.448$, $\gamma_\mathrm{L}/\omega_0 = 1.824$, $\Delta\varepsilon_\mathrm{L}/\omega_0 = 1.672$ and $\omega_0 = 10^{15}\,s^{-1}$.

II. MULTILAYER STRUCTURES CONSIDERED

In the main text, we consider a multilayer with five unit cells, see Fig. 1 of the main text. Here we show that the same phenomena can also be observed in analogous structures with only two unit cells, that are easier to fabricate and where the gain layers can more easily be pumped. We consider two multilayer structures, which we call M1 and M2:

M1: Multilayer with lossy a-layers and amplifying b-layers, $d_\mathrm{a} = 6\,\mathrm{nm}$ and $d_\mathrm{b} = 60\,\mathrm{nm}$, with dielectric functions described by Eqs. (1) and (2), respectively. Two unit cells, total thickness 132 nm.

M2: As previous, but now with $d_\mathrm{a} = d_\mathrm{b} = 6\,\mathrm{nm}$. Total thickness 24 nm.

Given the experimental values for gain and loss, where gain levels are typically smaller than loss, exact loss compensation can occur only in M1, as we shall see, where gain layers are considerably thicker than the lossy metal layers. Thicker layers are easier to pump, which is an advantage, but there is a tradeoff here, since still the unit cell should be subwavelength for effective-medium theories to be meaningful.

III. EFFECTIVE-MEDIUM PARAMETERS

As stated in the main text, we compare two independent methods to determine effective material parameters, namely a volume-averaging method producing an ε_ave on the one hand, and on the other hand an effective ε_eff retrieved from an S-matrix method, where the S-matrix contains the complex transmission and reflection amplitudes of the metamaterial. We first describe both methods in some more detail:

Volume-averaging method.— As is well known, multilayer metamaterials in general are anisotropic effective media, with different effective dielectric functions perpendicular and parallel to the layers. We only consider propagation perpendicular to the layer, *i.e.* in the $\hat{z}$-direction, in which case we only need to consider the in-plane effective dielectric tensor element given by [11, 12]

$$\varepsilon_\mathrm{ave} = p_\mathrm{a}\,\varepsilon_\mathrm{a} + p_\mathrm{b}\,\varepsilon_\mathrm{b}, \tag{3}$$

in terms of the volume fractions $p_\mathrm{a} = d_\mathrm{a}/(d_\mathrm{a} + d_\mathrm{b})$ and $p_\mathrm{b} = 1 - p_\mathrm{a}$. Thus $\varepsilon_\mathrm{ave} = n_\mathrm{ave}^2$ is simply the volume average of the dielectric functions of the layers.

S-matrix method.— Here the effective permittivity and index are obtained by stating that the metamaterial effectively has the same transmission and reflection properties as a homogeneous slab of the same thickness and with the effective index n_eff of the metamaterial. The latter is the unknown, which can be determined from reflection and transmission amplitudes in the multilayer's S-matrix as [13]

$$\sqrt{\varepsilon_\mathrm{eff}} = n_\mathrm{eff} = \pm\left[\frac{\cos^{-1}[1 - r^2 + t'^2]/(2t')}{\omega d/c}\right] + \frac{2\pi m}{\omega d/c}, \tag{4}$$

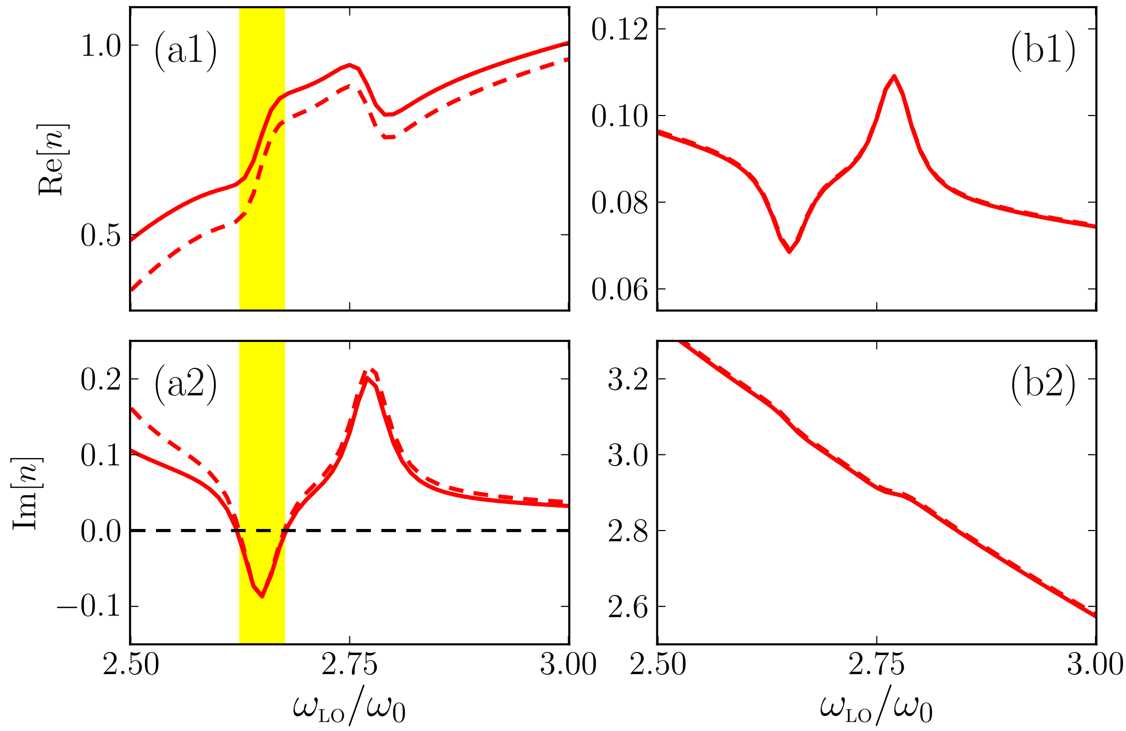

FIG. 1: Real and imaginary parts of the effective refractive indices $n_{\rm ave}$ (dashed lines) and $n_{\rm eff}$ (solid lines), defined in Eqs. (3) and (4), respectively. Dielectric functions for the amplifying and lossy layers are described by Eqs. (1) and (2), respectively. The frequency range considered corresponds to a free-space wavelength interval from 753 nm down to 629 nm. Panels (a1, a2): multilayer M1, $d_{\rm a} = 6\,{\rm nm}$ and $d_{\rm b} = 60\,{\rm nm}$. The frequency interval with net gain is highlighted in yellow; Panels (b1, b2): multilayer M2, $d_{\rm a} = d_{\rm b} = 6\,{\rm nm}$. The $n_{\rm eff}$ and $n_{\rm ave}$ agree so well that solid and dashed lines overlap.

where m is an integer that equals zero for the subwavelength structures that we consider.

In this supplement in Fig. 1, for completeness we illustrate the agreement of the effective-indices $n_{\rm ave}$ and $n_{\rm eff}$ for the multilayers M1 and M2. As one can see, the agreement for M1 (unit cell thickness 66 nm) the agreement is reasonably good, especially in the region of interest with (almost) complete loss compensation, while for M2 (unit cell thickness 12 nm), the agreement is excellent. For the multilayers considered in the main text, with unit cell thicknesses also of 12 nm, we found that these two methods to determine effective parameters likewise show excellent agreement.

Fig. 1 also shows that only for M1 does it occur that Im$[n]$ vanishes. This exact loss compensation occurs at two specific frequencies, similar to what was found for the single-resonance models in the main text, in Fig. 3(a). In Fig. 1 these frequencies correspond to the low- and high-frequency end points of the interval highlighted in yellow where net gain occurs. There are two main difference with the loss-compensating structure of the main text: first, the amplifying layers of M1 are quite a lot thicker than the metal ones. Second, whereas for the model in the main text net gain was found outside a finite frequency interval, here in the more realistic model, net gain is found within a narrow frequency interval only, around the resonance frequencies of the dye molecules that produce gain when pumped.

For M2 the gain layers are as thick as the lossy ones, as in the model used in the main text. In contrast to the multilayer of the main text, in M2 the more realistic gain described by Eq. (1) is considerably smaller than the loss of Eq. (2). Some – but by far not all – of the loss in the silver layers is compensated by the amplifying dye layers. The net effect is that the effective medium corresponding to M2 is still quite lossy, as Fig. 1(b2) illustrates.

IV. QUADRATURE VARIANCE

The quadrature variance of the light entering the homodyne detector has thee distinct contributions. One contribution solely depends on the light entering from the right, described by the squeezed input state $|R\rangle$, which is partially reflected into the detector. Another contribution solely depends on the light entering from the left, described by the

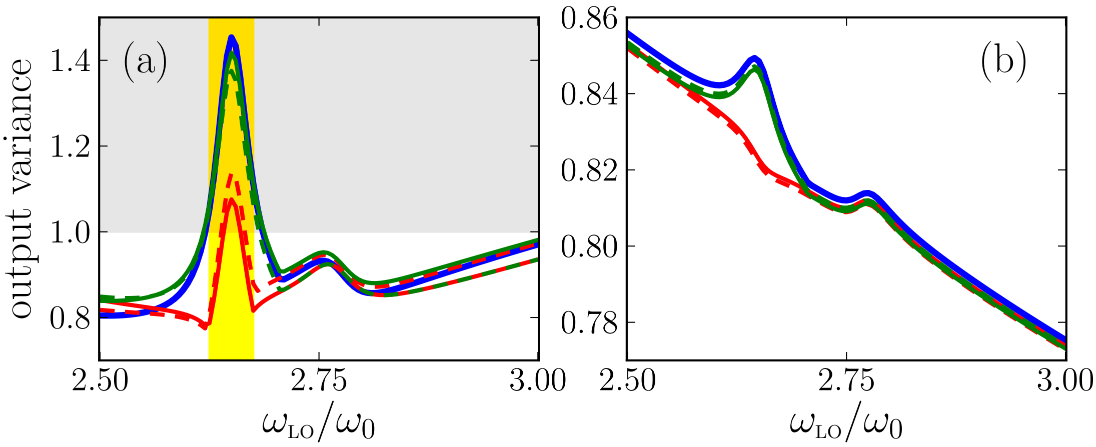

FIG. 2: Output quadrature variances of the light entering the homodyne detector, computed with exact multilayer theory (blue solid line), effective index theory using n_{eff} (red solid lines), effective-index theory using n_{ave} (red dashed lines), QOEM theory using n_{eff} (green solid lines), and finally QOEM theory using n_{ave} (green dashed lines). Panel (a): multilayer M1. The frequency interval with net gain is highlighted in yellow, as in Fig. 1(a2); panel (b): multilayer M2. Both here and in the main text, the incident squeezed states $|\mathrm{L},\mathrm{R}\rangle$ have strengths $\xi_{\mathrm{L}} = \xi_{\mathrm{R}} = 0.2$ and phases $\phi_{\mathrm{L}} = 2\phi_{\mathrm{LO}} - 2$ and $\phi_{\mathrm{R}} = 2\phi_{\mathrm{LO}} - 5$.

squeezed input state $|L\rangle$, which is partially transmitted into the detector. These first two contributions only rely on the classical homogenization theory to produce the 2×2 matrix A_{eff} introduced in the main text. This matrix is the same in the usual effective-medium theory and in the QOEM theory. The third and final contribution to the output quadrature variance is the quantum noise, which is independent of the optical input states $|L, R\rangle$ but depends instead on the (thermally distributed) internal material states of all lossy and amplifying layers. By choosing squeezed input states of light, the relative contribution of the quantum noise to the output variance is enhanced. The usual effective-index theory and the QOEM theory differ in their predictions of the output quadrature variance due to quantum noise, as discussed in the main text.

We compute the total quadrature variances of the output state of light that enters the homodyne detector. We compare the exact multilayer theory and two effective-medium theories. The latter two are introduced in the main text, namely the usual effective-index theory, and our quantum optical effective-medium (QOEM) theory that features the effective noise photon distribution of Eq. (7) as an additional effective parameter. Moreover, we can choose which of the two effective indices n_{ave} and n_{eff} to use in the two effective-medium theories. So there are five graphs to show, and this we do in Fig. 2, in panel (a) for multilayer M1 and in panel (b) for M2.

Fig. 2(a) for M1 shows that the usual effective-index theory breaks down and the QOEM theory is accurate in describing the variance of the light emerging from the loss-compensating metamaterial. As for the model calculations in the main text, the differences between the effective-medium theories are considerable. Also for M1 do we find frequencies for which the effective-index theory incorrectly predicts squeezing of the output light whereas the exact calculations and our QOEM theory predict no squeezing (variance > 1, in the grey area).

In both effective-medium theories, there are only small differences depending on whether one uses n_{eff} or n_{ave} as the effective index, as one can see by comparing the solid red curves with the dashed red ones, and the solid green curves with the dashed green ones. These small differences do not affect our main conclusions about M1 that the usual effective-index theory breaks down and the QOEM theory is accurate.

Fig. 2(b) shows the analogous graphs for the multilayer M2. Although only a fraction of the loss is compensated for, recall Fig. 1(b2), the output light stays squeezed both according to the exact calculation and to the two effective-medium theories. The reason is that the total thickness of the metamaterial is only 24 nm, which gives only a small fraction of reflection and especially the amount of quantum noise is consequently small. Nevertheless, it is clear that also for M2 the exact theory is well approximated by the QOEM theory but not by effective-index theory. Differences between n_{ave} and n_{eff} are so small for M2 [recall Fig. 1(b)] that it really does not matter which of the two values ones uses to calculate the variances, as Fig. 2(b) illustrates. The same is true for the five-period multilayer structure considered in the main text.

V. CONCLUSIONS

In this supplementary material we showed that the usual effective-medium theory breaks down for loss-compensated metamaterials, and our quantum optical effective-medium theory is accurate, also when using measured values for dielectric functions of gain and loss materials. We thus observe the same qualitative behavior as for the simple single-Lorentzian dielectric functions used in the main text. This supports our claim that we identify a fundamental issue about loss compensation in quantum optics that has observable consequences.

In experiments, gain is typically smaller than loss, so layers of gain materials should be chosen thicker than the lossy layers to obtain complete loss compensation. We illustrated this by considering two multilayer metamaterials, one with layers with unequal thickness (M1) and one with gain and loss layers of the same thickness (M2).

For the experimental values of amplifying and lossy dielectric functions, we find reasonably good (M1) and excellent (M2) agreement over a large frequency range for the effective refractive indices computed with two independent methods, S-matrix based ε_{eff} versus volume-average ε_{ave}. How well these effective parameters agree is a typical problem studied in classical-optics metamaterial research. Both for M1 and for M2, our predicted output variances show that choosing either classical or quantum optical effective-medium theories gives a significant difference for loss-compensated metamaterials, whereas choosing either ε_{eff} or ε_{ave} matters much less. Both for M1 and M2, only the QOEM theory agrees well with exact quantum optical calculations for multilayers.

---

[1] A. A. Govyadinov and V. A. Podolskiy, Phys. Rev. Lett. **97**, 223902 (2006).
[2] S. Xiao, V. P. Drachev, A. V. Kildishev, X. Ni, U. K. Chettiar, H-K. Yuan and V. M. Shalaev, Nature, **466**, 735 (2010).
[3] S. Wuestner, A. Pusch, K. L. Tsakmakidis, J. M. Hamm and O. Hess, Phys. Rev. Lett. **105**, 127401 (2010).
[4] J. M. Hamm, S. Wuestner, K. L. Tsakmakidis, and O. Hess, Phys. Rev. Lett. **107**, 167405 (2011).
[5] P. Sperber, W. Spangler, B. Meier, and A. Penzkofer, Opt. Quantum. Electron. **20**, 395 (1988).
[6] I. De Leon and P. Berini, Phys. Rev. B, **78**, 161401(R) (2008).
[7] I. De Leon and P. Berini, Opt. Express **17**, 20191 (2009).
[8] I. De Leon and P. Berini, Nature Phot. **4**, 382 (2010).
[9] S. G. Rodrigo, F. J. Garcia-Vidal, and L. Martin-Moreno, Phys. Rev. B **77**, 075401 (2008).
[10] J. M. McMahon, Y. Wang, L. J. Sherry, R. P. van Duyne, L. D. Marks, S. K. Gray, and G. C. Schatz, J. Phys. Chem. C **113**, 2731 (2009).
[11] D. J. Bergman, Phys. Rep. **43**, 377 (1978).
[12] B. Wood, J. B. Pendry, and D. P. Tsai, Phys. Rev. B **74**, 115116 (2006).
[13] D. R. Smith, S. Schultz, P. Markoš, and C. M. Soukoulis, Phys. Rev. B **65**, 195104 (2002).